Journal of Solid Mechanics Vol. 4, No. 2 (2012) pp. 128-143

Small Scale Effect on the Vibration of Orthotropic Plates Embedded in an Elastic Medium and Under Biaxial In-plane Pre-load Via Nonlocal Elasticity Theory

M. Mohammadi[1], M. Goodarzi[1], M. Ghayour[2,*], S. Alivand[1]

[1]*Department of Engineering, Ahvaz branch, Islamic Azad university, Ahvaz, Iran*
[2]*Department of Mechanical Engineering, Isfahan University of Technology, Isfahan 84156-83111, Iran*

Received 6 February 2012; accepted 8 April 2012

ABSTRACT

In this study, the free vibration behavior of orthotropic rectangular graphene sheet embedded in an elastic medium under biaxial pre-load is studied. Using the nonlocal elasticity theory, the governing equation is derived for single-layered graphene sheets (SLGS). Differential quadrature method (DQM) has been used to solve the governing equations for various boundary conditions. To verify the accuracy of the present results, a Navier's approach is also developed. DQM results are successfully verified with those of the Navier's approach. The results are subsequently compared with valid result reported in the literature. The effects of the small scale, pre-load, Winkler and Pasternak foundations and material properties on natural frequencies are investigated. The results are shown that with the decrease of in-plane pre-loads the curves isotropic and orthotropic non-dimensional frequency in approaches close to each other.

Keywords: Nonlocal elasticity theory; Vibration; Biaxial in-plane pre-load; Orthotropic Nanoplates ; Pasternak foundation

1 INTRODUCTION

IN the past decade, the attention of scientific community international has carried to the investigation of the behavior of matters at the atomic scale of material. The growth of scientists at this length scale has carried to the creating of the phrase nanotechnology. Nanotechnology is studied as one of the most encouraging technologies to be researched now. This technology could have enormous influence on information technology, aerospace, electronic devices, defense production and medical devices. Many endeavors have been made to construct nanodevices, expand and utilize matters on the nano scale. Some encouraging utilization have commenced to appear. One of the best examples of novel nanostructures are carbon nanotubes (CNT). Carbon nanotubes are allotropes of carbon. These are derived by bottom-up chemical synthesis processes. In carbon nanotubes, the chemical compound and atomic bonding configuration is simple. However, these materials represent various structure-property relations among the materials. Since the carbon nanotubes [1] are discovered, a large number of researcher have studied this material due to their mechanical properties (strength, stiffness), electrical and thermal properties. A single-walled nanotube (SWNT) can be formed by rolling a sheet of graphene into a cylinder along an {m, n) lattice vector in the graphene plane. In recent years, carbon nanotube have been used as actuators, charge detection devices, parametric amplifiers biosensors [2], nanorelays and nano electromechanical switches [3]. By using of continuum mechanics

*Corresponding author. Tel.: +98 9369712728.
E-mail address: m.ghayour.iut@gmail.com (M.Ghayour).

model and molecular dynamic simulations, the mechanical behaviors of nanostructures have been widely studied [4, 5]. Continuum mechanics in comparison to the molecular dynamic has been widely investigated for mechanical properties of two dimensional nanostructures, because the molecular dynamic is computationally expensive. It is admirable to expand continuum theories that may overcome the limitations of atomistic simulations regarding length scales. Newly, the continuum mechanics approximation has been widely and successfully utilized to investigate the mechanical behavior of CNTs, such as the stability analysis [6], free vibration [7, 8, 9], thermo-mechanical analysis of CNTs [10], because in many applications, the results from continuum mechanics approximation are exactly matched with the other results of the atomistic approaches [11]. The nonlocal elasticity theory has been used to investigate screw dislocation and surface waves in solids [12]. In the nonlocal elasticity theory, the size effects are captured by assuming the stress components at a given point dependent on the strain component at all points in the domain.

It is cleared that the natural frequency is easily affected by the applied in-plane load. As a result, the effect of in-plane load on the property of out of plane vibration of graphene sheet is of practical interest. Number of researches have been investigated on the nonlocal graphene sheets very limited compared with one-dimensional nonlocal nanostructures (nanobeams, nanowire, nanoring and nanorods). Pradhan and Murmu [13] investigated buckling of single layer graphene sheet by nonlocal elasticity theory. They have shown that the difference in behavior between uniaxial and biaxial compressions decreases as the size of the graphene sheets increases. using nonlocal elasticity theory, Pradhan [14] investigated buckling of single layer graphene sheet based on third order shear deformation theory. He reported that the variation of buckling load ratio is insignificant with the change in elastic modulus and thickness of the graphene sheet. Murmu and Pradhan [15] used nonlocal elasticity theory for vibration behavior of nano-single-layered graphene sheets embedded in elastic medium. Their numerical results are shown that the fundamental frequencies depend significantly on the moduli of the surrounding medium. Pradhan and Phadikar [16] investigated the vibration of embedded multilayered graphene sheets based on nonlocal continuum models. Aghababaei and Reedy [17] developed third-order shear deformation plate theory for bending and vibration of rectangular nanoplate based on nonlocal elasticity theory. Pradhan and Murmu [18] investigated buckling of nanoplate under biaxial compression load. They assumed rectangular nanoplate with isotropic properties and without elastic medium also they investigated stability of nanoplate under compression pre-load. Murmu and pradhan [19] studied biaxially compressed orthotropic plates based on nonlocal parameter. They proposed explicit expressions for the non-dimensional buckling load for the nanoplate with all edge simply supported but they didn't investigate the effect of boundary conditions and the elastic medium on the non-dimensional buckling load. Murmu and Pradhan [20] represented vibration analysis of nanoplates under uniaxial prestressed conditions via nonlocal elasticity but they didn't consider elastic medium whereas in nature, a single-layered rectangular graphene sheet embedded in a polymer matrix. They assumed rectangular nanoplate with isotropic properties whereas it has been reported that the graphene sheets have orthotropic properties [4]. In addition, they didn't investigate the effect of biaxial preload and tensile preload on the non-dimensional frequency. Some researches of the nanoplates have been reported on the mechanical properties. However, compared to the nanotubes, studies for the nanoplates are very limited, particularly for the vibration properties under pre-stressed.

In the present study, we emphasize much on orthotropicity of plates because nanoplates such as graphene sheets (GS) is reported to be possessing orthotropic properties [4]. The effect of polymer matrix on the frequency vibration and the non-dimensional buckling load of rectangular nanoplate are considered. In other hand, the effect of tensile and compressive biaxial preloads on the vibration analysis is studied. The governing equations of motion are derived using the nonlocal elasticity theory. Differential quadrature method (DQM) is used to solve the governing equations for simply supported boundary conditions, clamped boundary conditions and various combinations of them. To verify the accuracy of the DQM solutions, the governing equation is also solved by the Navier's approach. The predicted results by the DQ technique are successfully verified with which those of the Navier's approach. From the results, some new and absorbing phenomena can be observed. To suitably design nano electro-mechanical system and micro electro-mechanical systems (NEMS/MEMS) devices using graphene sheets, the present results would be useful.

2 NONLOCAL PLATE MODEL

By using nonlocal elasticity theory, stress components for a linear homogenous nonlocal elastic body without the body forces are [12]:

$$\sigma_{ij}(x) = \int \lambda\left(\left|x - x'\right|, \mu\right) C_{ijkl}\varepsilon_{kl}(x')dV(x'), \qquad \forall x \in V, \tag{1}$$

where σ_{ij}, ε_{ij} and C_{ijkl} are the stress, strain and fourth order elasticity tensors, respectively. The integration extends over the entire body volume V. The function λ is the nonlocal modulus, which contains the small scale effects. It is obvious that the nonlocal modulus has the dimension of $\left(length\right)^{-3}$. μ is a material constant $(\mu = e_0 a / l)$ that depends on the internal a and external characteristics lengths l. Choice of the value of parameter e_0 is vital for the validity of nonlocal models. Hence, the effects of small scale and atomic forces are considered as material parameters in the constitutive equation. This parameter was determined by matching the dispersion curves based on the atomic models. The term $\left|x - x'\right|$ represents the distance between the two points (x and x').The differential form of Eq. (1) can be written as [17]:

$$\left(1 - \left(e_0 l_i\right)^2 \nabla^2\right)\sigma^{nl} = \left[C\right]\left\{\varepsilon\right\} \tag{2}$$

where σ^{nl}, ε, denote the nonlocal stress and the strain vector, respectively. C denote the elastic stiffness tensor. ∇^2 is the Laplacian operator in Cartesian coordinates and can be express as $\nabla^2 = (\partial^2 / \partial x^2 + \partial^2 / \partial y^2)$. In present research, we investigated nano monolayer orthotropic graphene sheets. In two-dimensional forms, Eq. (2) are expressed as [10]:

$$\begin{Bmatrix} \sigma_{xx}^{nl} \\ \sigma_{yy}^{nl} \\ \sigma_{xy}^{nl} \end{Bmatrix} - (e_0 l_i)^2 \nabla^2 \begin{Bmatrix} \sigma_{xx}^{nl} \\ \sigma_{yy}^{nl} \\ \sigma_{xy}^{nl} \end{Bmatrix} = \begin{bmatrix} E_1/(1-\upsilon_{12}\upsilon_{21}) & \upsilon_{12}E_2/(1-\upsilon_{12}\upsilon_{21}) & 0 \\ \upsilon_{12}E_2/(1-\upsilon_{12}\upsilon_{21}) & E_2/(1-\upsilon_{12}\upsilon_{21}) & 0 \\ 0 & 0 & 2G_{12} \end{bmatrix} \begin{Bmatrix} \varepsilon_{xx} \\ \varepsilon_{yy} \\ \varepsilon_{xy} \end{Bmatrix} \tag{3}$$

where E_1, E_2 are the Young's modulus, G_{12} is shear modulus, υ_{12}, υ_{21}, indicate Poisson's ratio, respectively. The strains in terms of displacement components in the middle surface can be written [15]:

$$\varepsilon_{xx} = -z\frac{\partial^2 w}{\partial x^2}, \quad \varepsilon_{yy} = -z\frac{\partial^2 w}{\partial y^2}, \quad \varepsilon_{xx} = -z\frac{\partial^2 w}{\partial x \partial y} \tag{4}$$

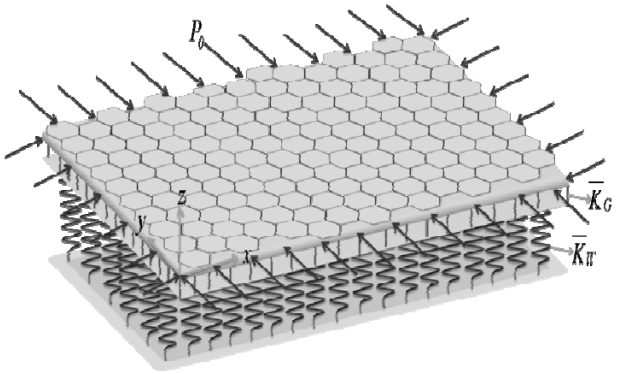

Fig.1
Rectangular nanoplate embedded in an elastic medium.

where the terms with w represent the strain components due to bending. The quantities $\partial^2 w/\partial x^2$ and $\partial^2 w/\partial y^2$ are the bending curvatures in x and y direction respectively, and $\partial^2 w/\partial x\partial y$ is the twist curvature. Thus, appropriate stress resultants for the plate theory are bending and twisting moment per unit length as defined as below for development of rectangular nanoplate [15]:

$$M_{xx} = \int_{-h/2}^{h/2} z\sigma_{xx}^{nl} dz \quad , \quad M_{yy} = \int_{-h/2}^{h/2} z\sigma_{yy}^{nl} dz \quad , \quad M_{xy} = \int_{-h/2}^{h/2} z\sigma_{xy}^{nl} dz, \tag{5}$$

Also, shear resultant Q_x and Q_y per unit length corresponding to the transverse shear nonlocal stresses σ_{xz}^{nl} and σ_{yz}^{nl} respectively and expressed as:

$$Q_x = \int_{-h/2}^{h/2} \sigma_{xz}^{nl} dz \quad , \quad Q_y = \int_{-h/2}^{h/2} \sigma_{yz}^{nl} dz, \tag{6}$$

Here, h is indicated as the thickness of the plate. By inserting Eq. (3), and Eq. (4) into Eq. (5) we can express stress resultants in terms of lateral deflection on the classical plate theory for the rectangular nanoplate as follows [15]:

$$\begin{aligned} &M_{xx} - (e_0 l_i)^2 \nabla^2 M_{xx} = -D_{11}\frac{\partial^2 w}{\partial x^2} - D_{12}\frac{\partial^2 w}{\partial y^2} \quad , \quad M_{yy} - (e_0 l_i)^2 \nabla^2 M_{yy} = -D_{12}\frac{\partial^2 w}{\partial y^2} - D_{22}\frac{\partial^2 w}{\partial x^2} \\ &M_{xy} - (e_0 l_i)^2 \nabla^2 M_{xy} = -2D_{66}\frac{\partial^2 w}{\partial x \partial y}, \end{aligned} \tag{7}$$

D_{ij} is known as the different flexural rigidity of the orthotropic rectangular nanoplte and are defined as:

$$\left(D_{11},\, D_{12},\, D_{22},\, D_{66}\right) = \int_{-h/2}^{h/2} \left(E_1/(1-\upsilon_{12}\upsilon_{21}),\ \upsilon_{12}E_2/(1-\upsilon_{12}\upsilon_{21}),\ E_2/(1-\upsilon_{12}\upsilon_{21}),\ G_{12}\right) z^2 dz \tag{8}$$

Note that the relations given in Eq. (7) are in the nonlocal plate model and those reduce to that of the classical equation when the nonlocal parameter $(e_0 a)$ is set to zero. A mono-layered rectangular graphene sheet embedded in an elastic medium (polymer matrix) is shown in Fig. 1. For modelling polymer matrix, the Pasternak-type foundation model is studied which accounts for both normal pressure and the transverse shear deformation of the surrounding elastic medium. The equations of motion for the transverse vibration of an orthotropic rectangular nanoplate is expressed as [15]:

$$\frac{\partial M_{yy}}{\partial y} + \frac{\partial M_{xy}}{\partial x} - Q_y = 0 \tag{9a}$$

$$\frac{\partial M_{xx}}{\partial x} + \frac{\partial M_{xy}}{\partial y} - Q_x = 0 \tag{9b}$$

$$\begin{aligned} &\frac{\partial Q_x}{\partial x} + \frac{\partial Q_y}{\partial y} + f + N_{xx}\frac{\partial^2 w}{\partial x^2} + N_{yy}\frac{\partial^2 w}{\partial y^2} + 2N_{xy}\frac{\partial^2 w}{\partial x \partial y} - \overline{K}_W W \\ &+ \overline{K}_{Gx}\frac{\partial^2 w}{\partial x^2} + \overline{K}_{Gy}\frac{\partial^2 w}{\partial y^2} = m_0\frac{\partial^2 w}{\partial t^2} - m_2\left(\frac{\partial^4 w}{\partial x^2 \partial t^2} + \frac{\partial^4 w}{\partial y^2 \partial t^2}\right) \end{aligned} \tag{9c}$$

where $\overline{K}_W$ indicate the Winkler modulus, $\overline{K}_{Gx}$ and $\overline{K}_{Gy}$ are the shear modulus of the surrounding elastic medium. If the shear layer foundation stiffness is neglected, Pasternak foundation takes to Winkler foundation. If polymer matrix is homogeneous and isotropic, we will take $\overline{K}_{Gx} = \overline{K}_{Gy} = \overline{K}_G$. The term f denote transverse loading, m_0 and m_2 are mass moments of inertia and are defined as follows:

$$m_0 = \int_{-h/2}^{h/2} \rho dz, \quad m_2 = \int_{-h/2}^{h/2} \rho z^2 dz \tag{10}$$

where ρ denotes the density of the rectangular nanoplate. Using Eq. (9a) and Eq. (9b) to eliminate Q_x and Q_y from Eq. (9c) one can obtain

$$\begin{aligned} &\frac{\partial^2 M_{xx}}{\partial x^2} + \frac{\partial^2 M_{yy}}{\partial y^2} + 2\frac{\partial^2 M_{yy}}{\partial x \partial y} + f + N_{xx}\frac{\partial^2 w}{\partial x^2} + N_{yy}\frac{\partial^2 w}{\partial y^2} + 2N_{xy}\frac{\partial^2 w}{\partial x \partial y} - \overline{K}_W W \\ &+\overline{K}_{Gx}\frac{\partial^2 w}{\partial x^2} + \overline{K}_{Gy}\frac{\partial^2 w}{\partial y^2} = m_0\frac{\partial^2 w}{\partial t^2} - m_2\left(\frac{\partial^4 w}{\partial x^2 \partial t^2} + \frac{\partial^4 w}{\partial y^2 \partial t^2}\right). \end{aligned} \tag{11}$$

The substitution of Eq. (7) into the vibration equation of a nanoplate Eq. (11) yields the governing differential equation of orthotropic plates

$$\begin{aligned} &D_{11}\frac{\partial^4 w}{\partial x^4} + 2\left(D_{12} + 2D_{66}\right)\frac{\partial^4 w}{\partial x^2 \partial y^2} + D_{22}\frac{\partial^4 w}{\partial y^4} \\ &+\left(e_0 l_i\right)^2 \nabla^2 \begin{pmatrix} f + N_{xx}\dfrac{\partial^2 w}{\partial x^2} + N_{yy}\dfrac{\partial^2 w}{\partial y^2} + 2N_{xy}\dfrac{\partial^2 w}{\partial x \partial y} - m_0\dfrac{\partial^2 w}{\partial t^2} \\ +m_2\left(\dfrac{\partial^4 w}{\partial t^2 \partial x^2} + \dfrac{\partial^4 w}{\partial t^2 \partial y^2}\right) - \overline{K}_W W + \overline{K}_{Gx}\dfrac{\partial^2 w}{\partial x^2} + \overline{K}_{Gy}\dfrac{\partial^2 w}{\partial y^2} \end{pmatrix} \\ &-\begin{pmatrix} f + N_{xx}\dfrac{\partial^2 w}{\partial x^2} + N_{yy}\dfrac{\partial^2 w}{\partial y^2} + 2N_{xy}\dfrac{\partial^2 w}{\partial x \partial y} - m_0\dfrac{\partial^2 w}{\partial t^2} \\ +m_2\left(\dfrac{\partial^4 w}{\partial t^2 \partial x^2} + \dfrac{\partial^4 w}{\partial t^2 \partial y^2}\right) - \overline{K}_W W + \overline{K}_{Gx}\dfrac{\partial^2 w}{\partial x^2} + \overline{K}_{Gy}\dfrac{\partial^2 w}{\partial y^2} \end{pmatrix} = 0. \end{aligned} \tag{12}$$

The influence of the nonlocal parameter ($e_0 a$) in the governing equations take into account the changes that are caused by the decrease in the size of a body at small scale. The impression of size on the behavior of nanomaterials is named size effect. The local elasticity theory is independent from a scale factor so it cannot forecast the size effects. By nonlocal parameter, the governing equation is obtained from nonlocal continuum mechanics is changed in compression the classical equations from local continuum mechanics. This parameter ($e_o a$) is taken into the constitutive equations clearly as a material constant. At small scale, size effects can be prominent in the mechanical features of nanostructures. The size effect has important role in the static and dynamic details of nanostructures. This effect has shown by the molecular dynamics simulation and experimental investigation. Chen et al. [21] reported that, the nonlocal elasticity theory is logical physically as compression couple stress theory, micromorphic theory, Cosserat theory, etc.

3 PROBLEM SOLUTION

It is assumed that the plate is free from transverse loading $(f = 0)$ and the solution of the resulting equation is assumed to be harmonic with frequency (ω) [20]:

$$w(x,y,t) = W(x,y)e^{(i\omega t)} \tag{13}$$

We consider the plate subject to the in-plane compressive forces $N_{xx} = -\gamma_1 \overline{P_0}$, $N_{yy} = -\gamma_2 \overline{P_0}$, $N_{xy} = 0$ where γ_1 and γ_2 is constant. Using the Eq. (12), a non-dimensional nonlocal differential equation for vibration of orthotropic graphene sheet under biaxial preload and embedded in an elastic medium can be obtained

$$\begin{aligned}
&\frac{\partial^4 \mathrm{W}^*}{\partial\zeta^4} + 2\lambda_1\beta^2 \frac{\partial^4 \mathrm{W}^*}{\partial\zeta^2\partial\eta^2} + \lambda_2\beta^4 \frac{\partial^4 \mathrm{W}^*}{\partial\eta^4} \\
&+\mu^2 \left(\begin{array}{l}
-\gamma_1 P_0 \left(\dfrac{\partial^4 \mathrm{W}^*}{\partial\zeta^4} + \beta^2 \dfrac{\partial^4 \mathrm{W}^*}{\partial\zeta^2\partial\eta^2} \right) - \gamma_2 P_0 \left(\beta^4 \dfrac{\partial^4 \mathrm{W}^*}{\partial\eta^4} + \beta^2 \dfrac{\partial^4 \mathrm{W}^*}{\partial\zeta^2\partial\eta^2} \right) \\
+\Omega^2 \left(\dfrac{\partial^2 \mathrm{W}^*}{\partial\zeta^2} + \beta^2 \dfrac{\partial^2 \mathrm{W}^*}{\partial\eta^2} \right) - \Omega^2\varepsilon^2 \left(\dfrac{\partial^4 \mathrm{W}^*}{\partial\zeta^4} + 2\beta^2 \dfrac{\partial^4 \mathrm{W}^*}{\partial\zeta^2\partial\eta^2} + \beta^4 \dfrac{\partial^4 \mathrm{W}^*}{\partial\eta^4} \right) \\
-K_W \left(\dfrac{\partial^2 \mathrm{W}^*}{\partial\zeta^2} + \beta^2 \dfrac{\partial^2 \mathrm{W}^*}{\partial\eta^2} \right) + K_{Gx} \left(\dfrac{\partial^4 \mathrm{W}^*}{\partial\zeta^4} + \beta^2 \dfrac{\partial^4 \mathrm{W}^*}{\partial\zeta^2\partial\eta^2} \right) + K_{Gy} \left(\beta^4 \dfrac{\partial^4 \mathrm{W}^*}{\partial\eta^4} + \beta^2 \dfrac{\partial^4 \mathrm{W}^*}{\partial\zeta^2\partial\eta^2} \right)
\end{array} \right) \\
&+\gamma_1 P_0 \frac{\partial^2 \mathrm{W}^*}{\partial\zeta^2} + \gamma_2 P_0 \beta^2 \frac{\partial^2 \mathrm{W}^*}{\partial\eta^2} - \Omega^2 \mathrm{W}^* + \Omega^2\varepsilon^2 \left(\frac{\partial^2 \mathrm{W}^*}{\partial\zeta^2} + \beta^2 \frac{\partial^2 \mathrm{W}^*}{\partial\eta^2} \right) + K_W \mathrm{W}^* - K_{Gx} \frac{\partial^2 \mathrm{W}^*}{\partial\zeta^2} \\
&-K_{Gy}\beta^2 \frac{\partial^2 \mathrm{W}^*}{\partial\eta^2} = 0.
\end{aligned} \tag{14}$$

where non-dimensional frequency parameter and other terms are defined in the following form

$$\begin{aligned}
&\Omega_{mn} = \sqrt{\frac{\rho h}{D_{11}}}\omega_{mn} l^2, \quad \mu = \frac{e_0 a}{l}, \quad \beta = \frac{l}{b}, \quad \varepsilon = \frac{h}{\sqrt{12}l}, \quad \lambda_1 = \frac{D_{12} + 2D_{66}}{D_{11}}, \quad \lambda_2 = \frac{D_{22}}{D_{11}}, \mathrm{K}_W = \frac{\overline{K}_W l^4}{D_{11}}, \\
&\mathrm{K}_{Gx} = \frac{\overline{K}_{Gx} l^2}{D_{11}}, \quad \mathrm{K}_{Gy} = \frac{\overline{K}_{Gy} b^2}{D_{11}}, \quad \mathrm{P}_0 = \frac{\overline{P}_0 l^2}{D_{11}}, \quad \zeta = \frac{x}{l}, \quad \eta = \frac{y}{b}, \quad \mathrm{W}^* = \frac{W}{l}
\end{aligned} \tag{15}$$

3.1 Solution by DQM

DQM has been found to be an efficient numerical technique for the solution of initial and boundary value problems [22, 23, 24]. Consider a two dimensional field variable $u(x,y)$, the m-th order derivative of it with respect to x, and the $(m+n)-th$ order derivative of it with respect to x and y is approximated as [22]:

$$\left.\frac{\partial^m u}{\partial x^m}\right|_{(x_i,y_i)} = \sum_{k=1}^{N_x} C_{ik}^{(m)} u(x_k, y_j, t) = \sum_{k=1}^{N_x} C_{ik}^{(m)} u_{kj}(t) \tag{16a}$$

$$\left.\frac{\partial^{(m+n)} u}{\partial x^m \partial y^n}\right|_{(x_i,y_i)} = \sum_{k=1}^{N_x} C_{ik}^{(m)} \overline{C}_{jl}^{(n)} u(x_k, y_l, t) = \sum_{k=1}^{N_x} C_{ik}^{(m)} \overline{C}_{jl}^{(n)} u_{kl}(t) \tag{16b}$$

The method developed by Shu and Richard [25] is claimed to be computationally more accurate than other methods [26]. According to Shu and Richard rule [25], the weighting coefficients of the first-order derivatives in ζ direction ($\zeta = x$ or y) are determined as [25]:

$$C_{ij}^{(1)}=\begin{cases}\dfrac{M(\zeta_i)}{(\zeta_i-\zeta_j)M(\zeta_j)} & \text{for } i\neq j\\ -\sum\limits_{j=1,i\neq j}^{N_\zeta} C_{ij}^{(1)} & \text{for } i=j\end{cases} \qquad i,j=1,2,...,N_\zeta \tag{17}$$

where

$$M(\zeta_i)=\prod_{j=1,i\neq j}^{N_\zeta}(\zeta_i-\zeta_j) \tag{18}$$

In order to evaluate the weighting coefficients of higher-order derivatives, recurrence relations are derived as [25]:

$$C_{ij}^{(r)}=\sum C_{ik}^{(r-1)}C_{kj}^{(1)} \qquad \textit{and} \qquad 2\le r\le 4 \tag{19}$$

The natural and simplest choice of the grid points is equally spaced points in the direction of the coordinate axes of the computational domain. It was demonstrated that non-uniform grid points gives a better results with the same number of equally spaced grid points. In this paper, we choose these set of grid points in terms of natural coordinate directions ξ and η as [27]:

$$\begin{aligned}\xi_i &= \frac{1}{2}\left(1-\cos\left(\frac{(i-1)\pi}{(N-1)}\right)\right)\\ \eta_j &= \frac{1}{2}\left(1-\cos\left(\frac{(j-1)\pi}{(M-1)}\right)\right)\end{aligned} \quad \text{For} \quad \begin{aligned} i&=1,2,\ldots,N\\ j&=1,2,\ldots,M\end{aligned} \tag{20}$$

A rectangular GS is considered to be embedded in an elastic medium. The geometric properties of the GS are denoted by length *l,* width *b,* thickness *h*. Eq. (14) can be solved by DQM approach for various boundary conditions. The simply supported boundary conditions are mathematically represented as:

$$W^*=0,\quad \frac{\partial^2 W^*}{\partial\xi^2}=0,\ \text{at}\ \xi=0\ \text{and}\ \xi=1, \tag{21}$$

The clamped supported boundary conditions can be written as:

$$\begin{aligned} W^*&=0,\quad \frac{\partial W^*}{\partial\xi}=0,\ \text{at}\ \xi=0\ \text{and}\ \xi=1,\\ W^*&=0,\quad \frac{\partial W^*}{\partial\eta}=0,\ \text{at}\ \eta=0\ \text{and}\ \eta=1,\end{aligned} \tag{22}$$

The computational domain of the rectangular plate is $0\le\xi\le 1,\quad 0\le\eta\le 1$. Making use of Eqs. (16a-16b) and incorporating the boundary conditions by modified weighting coefficient method [26] we write Eq. (14) in non-dimensional form

$$\begin{aligned}
&\sum_{k=2}^{N-1} C_{ik}^{(4)} \mathrm{W}^*_{k,j} + 2\lambda_1\beta^2 \sum_{k1=2}^{N-1}\sum_{K2=2}^{M-1} C_{i,k1}^{(2)} \overline{C}_{j,k2}^{(2)} \mathrm{W}^*_{k1,k2} + \lambda_2\beta^4 \sum_{k=2}^{M-1} \overline{C}_{jk}^{(4)} \mathrm{W}^*_{i,k} \\
&-\mu^2\gamma_1 P_0 \left(\sum_{k=2}^{N-1} C_{ik}^{(4)} \mathrm{W}^*_{k,j} + \beta^2 \sum_{k1=2}^{N-1}\sum_{k2=2}^{M-1} C_{i,k1}^{(2)} \overline{C}_{j,k2}^{(2)} \mathrm{W}^*_{k1,k2} \right) - \Omega^2 \mathrm{W}^*_{i,j} \\
&-\mu^2\gamma_2 P_0 \left(\beta^4 \sum_{k=2}^{M-1} \overline{C}_{jk}^{(4)} \mathrm{W}^*_{i,k} + \beta^2 \sum_{k1=2}^{N-1}\sum_{k2=2}^{M-1} C_{i,k1}^{(2)} \overline{C}_{j,k2}^{(2)} \mathrm{W}^*_{k1,k2} \right) + K_W \mathrm{W}^*_{i,j} \\
&+\Omega^2\mu^2 \left(\begin{array}{l} \sum_{k=2}^{N-1} C_{ik}^{(2)} \mathrm{W}^*_{k,j} \\ +\beta^2 \sum_{k=2}^{M-1} \overline{C}_{jk}^{(2)} \mathrm{W}^*_{i,k} \end{array} \right) + \gamma_1 P_0 \sum_{k=2}^{N-1} C_{ik}^{(2)} \mathrm{W}^*_{k,j} + \gamma_2 P_0 \beta^2 \sum_{k=2}^{M-1} \overline{C}_{jk}^{(2)} \mathrm{W}^*_{i,k} \\
&-\Omega^2\varepsilon^2\mu^2 \left(\sum_{k=2}^{N-1} C_{ik}^{(4)} \mathrm{W}^*_{k,j} + 2\beta^2 \sum_{k1=2}^{N-1}\sum_{k2=2}^{M-1} C_{i,k1}^{(2)} \overline{C}_{j,k2}^{(2)} \mathrm{W}^*_{k1,k2} + \beta^4 \sum_{k=2}^{M-1} \overline{C}_{jk}^{(4)} \mathrm{W}^*_{i,k} \right) \\
&-K_W\mu^2 \left(\sum_{k=2}^{N-1} C_{ik}^{(2)} \mathrm{W}^*_{k,j} + \beta^2 \sum_{k=2}^{M-1} \overline{C}_{jk}^{(2)} \mathrm{W}^*_{i,k} \right) - K_{Gx} \sum_{k=2}^{N-1} C_{ik}^{(2)} \mathrm{W}^*_{k,j} - K_{Gy}\beta^2 \sum_{k=2}^{M-1} \overline{C}_{jk}^{(2)} \mathrm{W}^*_{i,k} \\
&+K_{Gx}\mu^2 \left(\sum_{k=2}^{N-1} C_{ik}^{(4)} \mathrm{W}^*_{k,j} + \beta^2 \sum_{k1=2}^{N-1}\sum_{k2=2}^{M-1} C_{i,k1}^{(2)} \overline{C}_{j,k2}^{(2)} \mathrm{W}^*_{k1,k2} \right) + \Omega^2\varepsilon^2 \left(\begin{array}{l} \sum_{k=2}^{N-1} C_{ik}^{(2)} \mathrm{W}^*_{k,j} \\ +\beta^2 \sum_{k=2}^{M-1} \overline{C}_{jk}^{(2)} \mathrm{W}^*_{i,k} \end{array} \right) \\
&+K_{Gy}\mu^2 \left(\beta^4 \sum_{k=2}^{M-1} \overline{C}_{jk}^{(4)} \mathrm{W}^*_{i,k} + \beta^2 \sum_{k1=2}^{N-1}\sum_{k2=2}^{M-1} C_{i,k1}^{(2)} \overline{C}_{j,k2}^{(2)} \mathrm{W}^*_{k1,k2} \right) = 0.
\end{aligned} \tag{23}$$

C and $\overline{C}$ are the weighting coefficient matrix in the x, y directions respectively. After implementation of the boundary conditions, Eq. (23) can be written in matrix form as:

$$[K_{total} - \Omega^2 I]\{\mathrm{W}^*\} = 0, \tag{24}$$

where I and Ω^2 are identity matrix and non-dimensional frequency described in Eq. (15). The Eq. (24) can be solved by a standard eigenvalue solver. Fig. 2 is shown flowchart of steps of DQ method.

3.2 Navier's approach

Exact solution of Eq. (14) can be solved for simply supported plate on all edges by using the Navier's approach. As in the case of free vibration of a rectangular nanoplate without any in-plane forces, the following solution can be seen to satisfy the simply supported boundary conditions of the plate [19]:

$$W(x,y) = \sum_{m=1}^{\infty}\sum_{n=1}^{\infty} W_{mn} \sin\left(\frac{m\pi x}{l}\right) \sin\left(\frac{n\pi y}{b}\right) \tag{25}$$

where m and n are the half wave numbers and W_{mn} is constant. By inserting Eq. (25) into Eq. (14), yields the non-dimensional natural frequency at small scale with various nanoplate properties, Winkler and shear elastic factors.

$$\Omega_{mn}^2 = \frac{\left(\begin{array}{l} \pi^4\left(m^4 + 2\lambda_1 m^2 n^2 \beta^2 + \lambda_2 n^4 \beta^4\right) + K_{Gy}\left(\pi^2\beta^4 n^2 + \mu^2\pi^4\left(\beta^6 n^4 + \beta^4 m^2 n^2\right)\right) \\ +K_{Gx}\left(\pi^2 m^2 + \mu^2\pi^4\left(m^4 + \beta^2 m^2 n^2\right)\right) + K_W\left(\mu^2\pi^2\left(m^2 + n^2\beta^2\right) + 1\right) \\ -P_0\left(\mu^2\pi^4\left(\gamma_1 m^4 + (\gamma_1 + \gamma_2)\beta^2 m^2 n^2 + \gamma_2 n^4\beta^4\right) + \pi^2\left(\gamma_1 m^2 + \gamma_2 n^2\beta^2\right)\right) \end{array} \right)}{\pi^2\left(m^2 + n^2\beta^2\right)\left(\varepsilon^2 + \mu^2\left(\varepsilon^2\pi^2\left(m^2 + n^2\beta^2\right) + 1\right)\right) + 1} \tag{26}$$

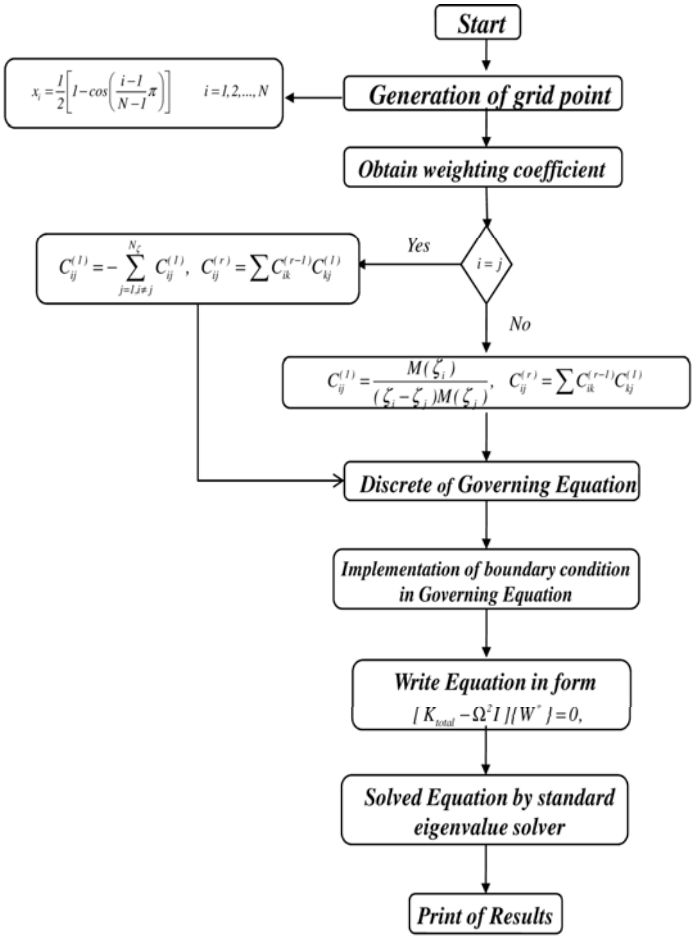

Fig.2
Flowchart of steps of applied DQ method.

It can be seen that Ω_{mn} reduces to zero as the magnitude P_0 of increases. When $\Omega_{mn}=0$, called the critical or buckling load, can be determined from Eq. (26) as:

$$\left(P_0\right)_{cr}=\frac{\left\{\begin{array}{l}\pi^4\left(m^4+2\lambda_1 m^2n^2\beta^2+\lambda_2 n^4\beta^4\right)+K_{Gy}\left(\pi^2\beta^4n^2+\mu^2\pi^4\left(\beta^6n^4+\beta^4m^2n^2\right)\right)\\+K_{Gx}\left(\pi^2m^2+\mu^2\pi^4\left(m^4+\beta^2m^2n^2\right)\right)+K_W\left(\mu^2\pi^2\left(m^2+n^2\beta^2\right)+1\right)\end{array}\right\}}{\mu^2\pi^4\left(\gamma_1m^4+\left(\gamma_1+\gamma_2\right)\beta^2m^2n^2+\gamma_2n^4\beta^4\right)+\pi^2\left(\gamma_1m^2+\gamma_2n^2\beta^2\right)} \tag{27}$$

From Eq. (27), it can be observed that if the Winkler and shear elastic factor are ignored, the buckling load will be reduced to Murmu and Pradhan [19]. Using Eq. (27), the frequency given by Eq. (26) can be expressed

$$\Omega_{mn}^2=\frac{\mu^2\pi^4\left(\gamma_1m^4+\left(\gamma_1+\gamma_2\right)\beta^2m^2n^2+\gamma_2n^4\beta^4\right)+\pi^2\left(\gamma_1m^2+\gamma_2n^2\beta^2\right)}{\pi^2\left(m^2+n^2\beta^2\right)\left(\varepsilon^2+\mu^2\left(\varepsilon^2\pi^2\left(m^2+n^2\beta^2\right)+1\right)\right)+1}\left[\left(P_0\right)_{cr}-P_0\right] \tag{28}$$

where Eq. (28) is the frequency equation orthotropic rectangular nanoplate under biaxial in-plane forces. And this frequency equation is for simply supported boundary conditions.

4 RESULTS AND DISCUSSION

In the present study, we investigated vibration of orthotropic rectangular nanoplate under in-plane load acting on edges and embedded in elastic medium. The scale coefficients are assumed smaller than 2.0 nm because these values for carbon nanotubes were taken by Wang and Wang [27] and Duan and Wang [28]. The materials properties of orthotropic rectangular graphene sheet are presented in Table 1.

Table 1
The materials properties of rectangular nanoplate.

Source	Material Properties of orthotropic of rectangular nanoplate				
	E_1 (Gpa)	E_2 (Gpa)	υ_{12}	υ_{21}	$\rho\ (kg/m^3)$
Ref. 4, 19	1765	1588	0.3	0.27	2300
	Material Properties of isotropic of rectangular nanoplate				
Ref. 18	E (Gpa)		υ		$\rho\ (kg/m^3)$
	1060		0.25		2250

The results of square isotropic nanoplates were compared with published data. Fig. 3 is shown Murmu and Pradhan's results [20], and the results obtained from this work for the free vibration problem of square isotropic nanoplates for case of uniaxial pre-stressed and without consider elastic medium. Here, nonlocal parameter and length of square nanoplate is considered 1nm, 10 nm respectively. It can be seen that the results herein exactly match with the other results reported.

As the results of DQ procedure depend on the number of grid points [23, 26], a convergence test is carried out. The non-dimensional frequencies of rectangular nanoplate are tabulated in Table 2. for various numbers of grid points and some values of nonlocal parameter. The table is plotted to obtain the minimum number of grid points required to determine accurate results. The length of rectangular nanoplate 10 nm is considered. It is assumed that the nanoplate subjected to compressive biaxial pre-load $P_0 = 10$. It can be easily seen form Table 2. that sixteen number of grid points along the ζ and η axes is sufficient in order to gain converge solution.

To study the effect of biaxial compressive pre-stressed on the non-dimensional frequency, in this section, the non-dimensional frequency versus compressive pre-load for isotropic and orthotropic properties of square nanoplate is shown in Fig. 4. The length of square nanoplate is 10 nm. It is found that non-dimensional frequency of the isotropic graphene sheet is always larger than that of orthotropic one. This is clear because plate with orthotropic properties is more flexible than that of isotropic one. From this figure, it is seen that nonlocal solution is smaller than classical (local) solution for all values of in-plane pre-load considered. Further, one could observe that effect initial compressive pre-load on non-dimensional natural frequency is important and nonlinear in nature. The natural frequencies decrease with increasing compressive in-plane pre-load and when the in-plane compressive kind pre-loads reach their critical value; the mode of vibration is buckled and the non-dimensional natural frequency become equal zero.

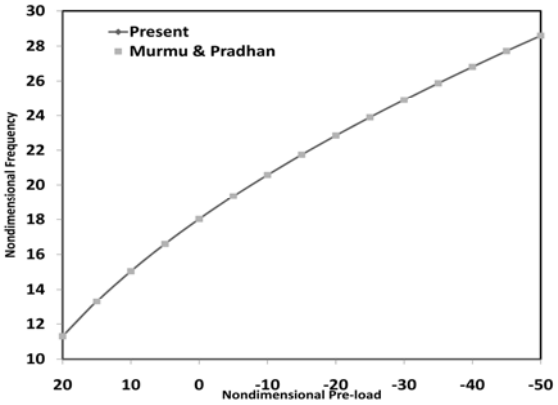

Fig.3
Comparison of results of fundamental frequencies obtained by the present study and that obtained by DQ approach.

Table 2
Validation and convergence study of differential quadrature method.

Number of grid point	e_0a (nm)									
	All edges simply supported					All edges clamped				
	0	0.5	1	1.5	2	0	0.5	1	1.5	2
10	13.4647	12.8879	10.9142	8.2097	4.0094	32.4663	31.0349	27.2614	22.1649	16.4095
12	13.4652	12.8879	10.9142	8.2097	4.0094	32.4616	31.0307	27.2584	22.1629	16.4084
14	13.4652	12.8879	10.9142	8.2097	4.0094	32.4608	31.0301	27.2578	22.1625	16.4081
16	13.4652	12.8879	10.9142	8.2097	4.0094	32.4608	31.0300	27.2578	22.1624	16.4080
18	13.4652	12.8879	10.9142	8.2097	4.0094	32.4608	31.0300	27.2578	22.1624	16.4080
20	13.4652	12.8879	10.9142	8.2097	4.0094	32.4608	31.0300	27.2578	22.1624	16.4080
Navier's approach	13.3304	12.6514	10.7640	7.8957	3.4937	-	-	-	-	-

The intersection points of the curves with the horizontal axis are the buckling load of nanoplate. The buckling load for isotropic graphene sheet is always more than buckling load for orthotropic graphene sheet. The buckling load kept on decreasing when the nonlocal parameter became larger. Therefore, the magnitudes of the in-plane compressive loads are important parameter for the design of a micro or nanoplate structures. Furthermore, the difference between the natural frequencies calculated by isotropic and orthotropic properties increases with decreasing nonlocal parameter. With the decreasing of in-plane pre-loads the curves isotropic and orthotropic in Fig. 4 approaches close to each other.

In Fig. 5 and Fig.6, we consider a mono-layered graphene sheet with isotropic and orthotropic properties. To investigate the influence in-plane stresses on the natural frequency in two cases compressive and tensile stresses, we define frequency fraction in non-dimensional natural frequencies with the in-plane stress to those without the in-plane stress as the following form

$$\textit{frequency}\ \text{fraction}=\frac{\text{nondimensional frequency with the inplane load}}{\text{nondimensional frequency without the inplane load}}$$

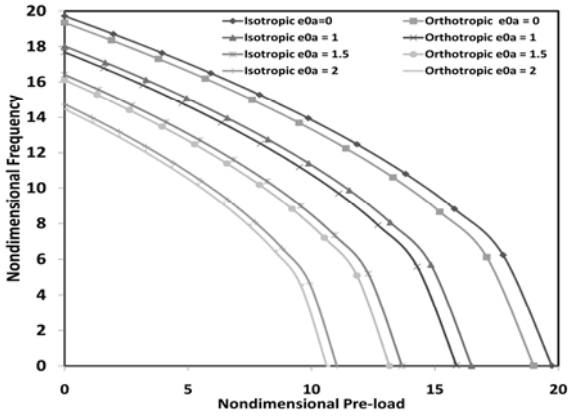

Fig.4
Change of non-dimensional frequency with non-dimensional pre-load for various nonlocal parameters.

The scale coefficient is 1 nm and the first mode number is considered. The in-plane loads are considered P_0=2, 4, 6, 8 and 10. In Fig. 5 frequency fraction is plotted versus aspect ratio for various compressive in-plane stresses. It is shown that the frequency fraction with different in-plane compressive loads will increase with the aspect ratio increasing. However, it is seen the non-dimensional frequency with in-plane compressive loads are smaller than the non-dimensional frequency without in-plane loads for all aspect ratio. This phenomenon is because compressive in-plane loads are caused to reduce of rigidity of nanoplate so the non-dimensional frequency of nanoplate with compressive in-plane loads is smaller than that for plate without in-plane preload. Then the frequency fraction for nanoplate with compressive in-plane preload is smaller than unit. It can also be observed that the frequency fraction will increas with the in-plane load decreasing. The plot of frequency fraction with respect to aspect ratio for the case of tensile in-plane stresses is demonstrated in Fig. 6. It is cleared; the behaviors of the frequency fractions for the

tensile in-plane loads are against compressive in-plane loads in Fig. 6. In the two case of in-plane loads (compressive and tensile loads), the effect of in-plane loads decreases with the increasing of aspect ratio. This means that at larger aspect ratio, the effect of in-plane load is less important.

In order to illustrate the effect of boundary condition on vibration response of the orthotropic graphene sheets under biaxial compressive pre-load $P_0 = 10$, six different boundary conditions are considered. For brevity, a four-letter symbol is used to denote the boundary conditions for the four edges of the nanoplate as follows:

SSSS: All edges simply supported.
SSSC: Simply supported along x =0, x = l and y = 0 and clamped along y = b.
SCCS: Simply supported along x = 0 and y = b and clamped along x = l and y =0.
SCCC: Simply supported along x = 0 and clamped along x = l, y = 0 and y = b.
CCCC: All edges clamped.

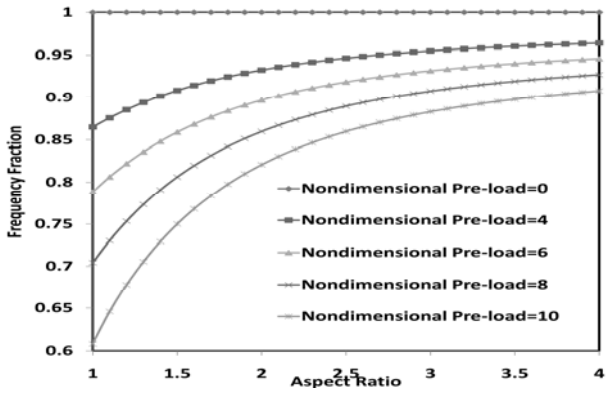

Fig.5
Change of frequency fraction with aspect ratio for various non-dimensional compressive pre-load.

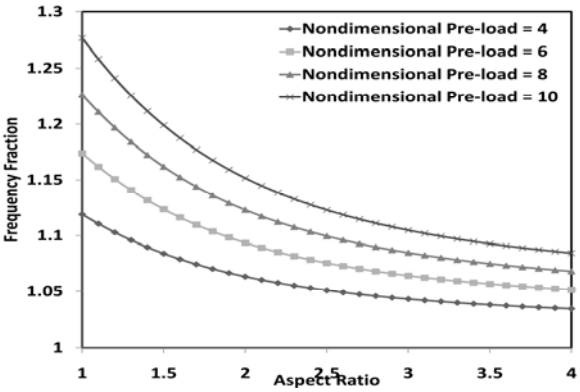

Fig.6
Change of frequency fraction with aspect ratio for various non-dimensional tensile pre-load.

Fig. 7 shows the variation of non-dimensional frequency with the length of nanoplate for the above-mentioned boundary conditions. As seen from the figure, the non-dimensional natural frequency also depends on the boundary conditions. The length of nanoplate is more noticeable for CCCC boundary condition when compared with SSSS boundary condition. This result can be explained as the rectangular nanoplate with clamped edges has more constraints than simply supported one. As the boundary conditions become more rigid, the non-dimensional natural frequency increases. Thus, the influence of length of nanoplate on the non-dimensional frequency of the orthotropic nanoplates for SSSS, SSSC, SCCS, SCCC and CCCC boundary conditions are in increasing order (CCCC > SCCC > SCCS > SSSC > SSSS). It is also found that the gap between any two curves approximately increases with increasing length of nanoplate.

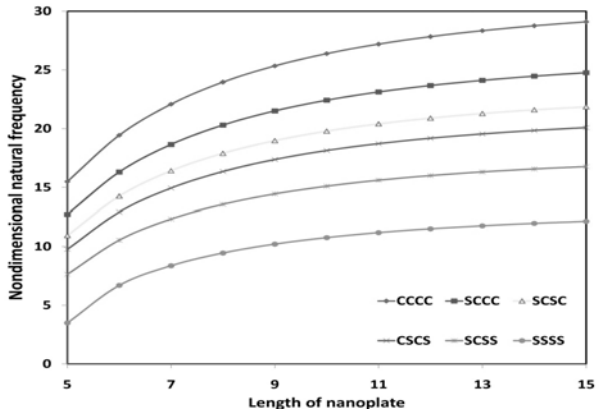

Fig.7
Change of natural frequency with length of nanoplate for various boundary conditions.

The effect of biaxial in-plane compressive load on the frequency of orthotropic graphene sheet embedded in an elastic medium is studied. The Winkler modulus parameter K_W , for the surrounding polymer matrix is gotten in the range of 0–400. We assumed that polymer matrix is homogeneous $K_{Gx} = K_{Gy} = K_G$. Then, shear modulus factor K_G is gotten in the range 0-10. Similar values of modulus parameter were also applied by Liew *et al*. [29]. The relationships between difference percent frequency versus Winkler constant K_W and shear modulus K_G for different in-plane stress and isotropic and orthotropic properties of graphene sheet are demonstrated in Figs. 8, 9. A scale coefficient e_0a = 2.0 nm is used in the analysis. The frequency difference percent is defined as

$$\text{Difference percent}=\left|\frac{frequency_{P=P_0}-frequency_{P=0}}{frequency_{P=0}}\right|\times 100$$

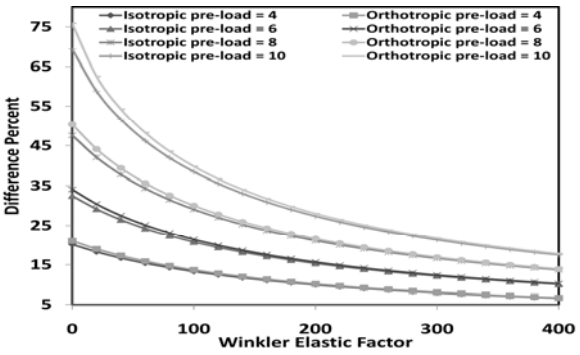

Fig.8
Change of difference percent with Winkler elastic factor for various non-dimensional pre-load.

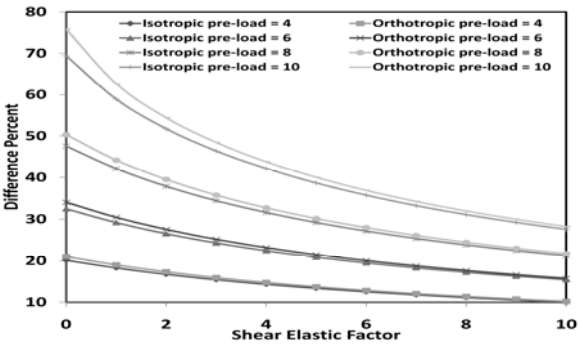

Fig.9
Change of difference percent with shear elastic factor for various non-dimensional pre-load.

As can be observed, the effect of in-plane pre-load on the non-dimensional natural frequency is less important for graphene sheet embedded in an elastic medium in compression with graphene sheet without elastic medium because the Winkler constant or shear modulus decreases then the effect of in-plane load on the difference percent increase. It can be observed for the consequences that the difference percent increases with increasing the in-plane stress. For larger in-plane stress, the decline of difference percent is quite important. It is cleared because the in-plane pre loads are caused to change in rigidity of nanoplate when the in-plane preload is grown the rigidity of nanoplate is more change. In other hand, when elastic factor increases, the rigidity of nanoplate increases and the effect of elastic factor on the rigidity of nanoplate is more than the effect of in-plane preload on that, consequently the gap between curves decreases and the effect of in-plane preload are reduced. So the slope of curve for nanoplate with larger in-plane preload are bigger than that for nanoplate with smaller in-plane preload. Also, the difference percent for orthotropic graphene sheet is larger than that for graphene sheet with isotropic properties. From these plots it is obvious the important influence of in-plane stress and elastic medium, in the cases isotropic and orthotropic graphene sheet on the non-dimensional frequency. Furthermore, the difference between the natural frequencies calculated by isotropic and orthotropic properties increases with decreasing Winkler and shear elastic factor.

To study the influence of Winkler and Pasternak foundation on the non-dimensional natural frequency and the non-dimensional buckling load of orthotropic rectangular nanoplates, the variation in non-dimensional natural frequency with the non-dimensional preload is shown in Fig. 10. The side of rectangular nanoplate, nonlocal parameter and aspect ratio is taken as 10 nm, 1 nm and 1 respectively. It is assumed that rectangular nanoplate is subjected to compressive in-plane preload. One could observe that the non-dimensional natural frequency increases with increase in Winkler and Pasternak parameter. In addition, it is clear that the nanoplate with larger Winkler and Pasternak parameter is need to more non-dimensional preload for that the nanoplate buckled. This phenomenon is because when the Winkler and Pasternak parameter increases the rigidity of nanoplate increases which leads to an increase in the non-dimensional buckling load and the non-dimensional natural frequency. Furthermore, it is clear that the effect of Pasternak parameter is more than the effect of Winkler parameter on the non-dimensional natural frequency and the non-dimensional preload.

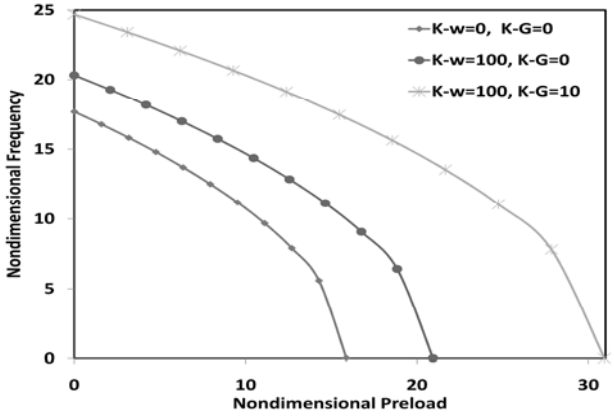

Fig.10
Change of non-dimensional frequency with non-dimensional pre-load for various Winkler and Pasternak parameter.

5 CONCLUSIONS

This study illustrates the importance of small scale effect on the vibration analysis of an orthotropic rectangular nanoplate under biaxial pre-load based on the nonlocal elasticity theory. It is shown that the nonlocal vibration frequencies are always smaller than the local solutions. Further, the non-dimensional frequency of the isotropic graphene sheet is always larger than that of orthotropic one. The frequency fraction decreases by increasing the compressive pre-load. In addition, the effect of in-plane loads decreases with the increasing of aspect ratio. The non-dimensional natural frequency becomes equal zero when the in-plane compressive pre-loads reach their critical value. The difference between two natural frequencies (the natural frequency calculated by isotropic and orthotropic properties) increases with decreasing nonlocal parameter and non-dimensional preloads. The behaviors of the frequency fractions for the tensile in-plane loads are against compressive in-plane loads. The non-dimensional

natural frequency increases when the boundary conditions become more rigid. The non-dimensional buckling load increases when the Winkler and Pasternak foundation increases. The Winkler constant or shear modulus factor increases as results the, effects of in-plane load on the difference percent, decreases. The difference between isotropic and orthotropic frequency increases with decreases in elastic factors (shear elastic and Winkler elastic factors).

ACKNOWLEDGEMENTS

The authors are grateful to Iranian Nanotechnology Development Committee for their financial support. They would also like to thank the referees for their useful comments.

REFERENCES

[1] Iijima S., 1991, Helical microtubules of graphitic carbon, *Nature* **354**: 56–58.
[2] Wang J., 2005, Carbon-Nanotube based electrochemical biosensors: *A Review, Electro Analysis* **17**: 7–14.
[3] Kinaret J.M., Nord T., Viefers S., 2003, A carbon-nanotube-based nanorelay, *Physics Letters A* **82**: 1287–1289.
[4] Reddy C.D., Rajendran S., Liew K.M., 2006, Equilibrium configuration and continuum elastic properties of finite sized grapheme, *Nanotechnology* **17**: 864–870.
[5] Sakhaeepour A., Ahmadian M., Vafai A., 2007, Applications of single-layered graphene sheets as mass sensors and atomistic dust detectors, *Solid State Communications* **145**: 168-172.
[6] Zhang Y.Q., Liu G.R., Han X., 2006, Effect of small length scale on elastic buckling of multi-walled carbon nanotubes under radial pressure, *Physics Letters A* **349**: 370–376.
[7] Aydogdu M., 2009, Axial vibration of the nanorods with the nonlocal continuum rod model, *Physica E* **41**: 861–864.
[8] Filiz S., Aydogdu M., 2010, Axial vibration of carbon nanotube heterojunctions using nonlocal elasticity, *Computational Materials Science* **49**: 619-627.
[9] Murmu T., Adhikari S., 2011, Nonlocal vibration of carbon nanotubes with attached buckyballs at tip, *Mechanics Research Communications* **38**: 62–67.
[10] Malekzadeh P., Setoodeh A.R, Alibeygibeni A., 2011, Small scale effect on the thermal buckling of orthotropic arbitrary straight-sided quadrilateral nanoplates embedded in an elastic medium, *Composite Structures* **93**: 2083-2089.
[11] Khademolhosseini F., Rajapakse R.K.N.D., Nojeh A., 2010, Torsional buckling of carbon nanotubes based on nonlocal elasticity shell models, *Computational Materials Science* **48**: 736–742.
[12] Eringen A.C., 1983, On differential of non-local elasticity and solutions of screw dislocation and surface waves, *Journal Applied Physic* **54**: 4703–4710.
[13] Pradhan S.C., Murmu T., 2009, Small scale effect on the buckling of single-layered graphene sheets under biaxial compression via nonlocal continuum mechanics, *Computational Materials Science* **47**: 268–274.
[14] Pradhan S.C., 2009, Buckling of single layer graphene sheet based on nonlocal elasticity and higher order shear deformation theory, *Physics Letters A* **373**: 4182–4188.
[15] Murmu, T. Pradhan, S.C., 2009, Vibration analysis of nano-single-layered graphene sheets embedded in elastic medium based on nonlocal elasticity theory, *Journal Applied Physic* **105**: 064319.
[16] Pradhan S.C., Phadikar J.K., 2009, Small scale effect on vibration of embedded multi layered graphene sheets based on nonlocal continuum models, *Physics Letters A* **373**: 1062–1069.
[17] Aghababaei R., Reddy J.N., 2009, Nonlocal third-order shear deformation plate theory with application to bending and vibration of plates, *Journal of Sound and Vibration* **326**: 277-289.
[18] Pradhan S.C., Murmu T., 2009, Small scale effect on the buckling of single-layered graphene sheets under biaxial compression via nonlocal continuum mechanics, *Computational Materials Science* **47**: 268–274.
[19] Murmu T., Pradhan S.C., 2009, Buckling of biaxially compressed orthotropic plates at small scales, *Mechanics Research Communications* **36**: 933–938.
[20] Murmu T., Pradhan S.C., 2009, Vibration analysis of nanoplates under uniaxial prestressed conditions via nonlocal elasticity, *Journal Applied Physic* **106**: 104301.
[21] Chen Y., Lee J.D., Eskandarian A., 2004, Atomistic viewpoint of the applicability of microcontinuum theories, *International Journal Solids Structure* **41**: 2085-2097.
[22] Bert CW., Malik M., 1996, Differential quadrature method in computational mechanics: a review, *Applied Mechanic Review* **49**: 1–27.
[23] Farajpour A., Shahidi A.R., Mohammadi M., Mahzoon M., 2012, Buckling of orthotropic micro/nanoscale plates under linearly varying in-plane load via nonlocal continuum mechanics, *Composite Structures* **94**: 1605–1615.
[24] Danesh M., Farajpour A., Mohammadi M., 2012, Axial vibration analysis of a tapered nanorod based on nonlocal elasticity theory and differential quadrature method, *Mechanics Research Communications* **39**: 23– 27.

[25] Shu C, Richards Be.,1992, Application of generalized differential quadrature to solve two-dimensional incompressible Navier Stokes equations, *International Journal for Numerical Methods in Fluids* **15**: 791–798.
[26] Shu C., 2000, *Differential Quadrature and its Application in Engineering*, Springer, Great Britain.
[27] Wang Q., Wang C.M., 2007, The constitutive relation and small scale parameter of nonlocal continuum mechanics for modelling carbon nanotubes, *Nanotechnology* **18**: 075702.
[28] Duan W.H., Wang C.M., 2007, Exact solutions for axisymmetric bending of micro/ nanoscale circular plates based on nonlocal plate theory, *Nanotechnology* **18**: 385704.
[29] Liew K., He M., X Q., Kitipornchai S., 2006, Predicting nanovibration of multi-layered graphene sheets embedded in an elastic matrix, *Acta Material* **54**: 4229-4236.